

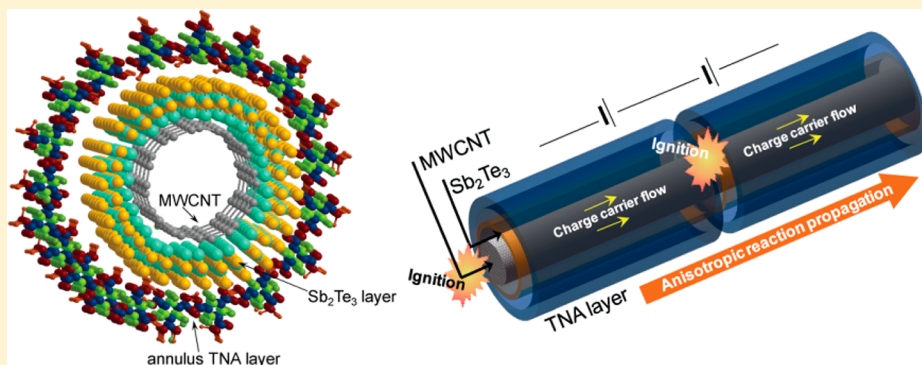
Enhanced Electrical Potential of Thermoelectric Power Waves by Sb₂Te₃-Coated Multiwalled Carbon Nanotube Arrays

Seunghyun Hong,^{†,‡} Wonyoung Kim,^{‡,§} Seong-Jae Jeon,^{||,⊥} Seong Chu Lim,[§] Hoo-jeong Lee,^{||} Seungmin Hyun,[†] Young Hee Lee,^{§,#} and Seunghyun Baik*,^{‡,§,§,▽}

[†]SKKU Advanced Institute of Nanotechnology (SAINT), [‡]Samsung-SKKU Graphene Center (SSGC), [§]Department of Energy Science, ^{||}School of Advanced Materials, [#]Institute of Basic Science, Center for Integrated Nanostructure Physics and BK21 Physics Division, and [▽]School of Mechanical Engineering, Sungkyunkwan University, Suwon, Korea

[⊥]Department of Nano-mechanics, Korea Institute of Machinery and Materials, Daejeon, Korea

Supporting Information



ABSTRACT: Thermoelectric power waves, where multiwalled carbon nanotubes coated with cyclotrimethylene trinitramine (MWCNT/TNA) directly convert chemical energy to electricity, have received considerable attention recently. However, the low Seebeck coefficient of carbon nanotubes has been regarded as a hurdle to increasing the electrical potential. Here, we present Sb₂Te₃-coated MWCNT arrays prepared by a sputtering method. An analytical model predicts an increase in Seebeck coefficient of the annular multishell structure by ~75%. The heterostructure coupled with exothermic chemical reaction of TNA demonstrates an increase in peak electrical potential of 175% (~198 mV), compared with typical outputs of bare MWCNT/TNA (~72 mV). A serial connection of two repeating units increased the peak potential by up to 406 mV.

INTRODUCTION

The increasing need for self-powered miniature electronic devices motivates the development of small-scale power sources.^{1–3} Micropower energy harvesters, such as piezoelectric and thermoelectric generators, have emerged as promising candidates.^{1–3} Thermoelectric systems, which convert heat to electricity, provide an opportunity for portable green energy sources that are simple and reliable.^{3–5} Recently, the concept of thermopower waves was introduced.^{6–8} The exothermic chemical reaction of energetic materials was guided and accelerated by one-dimensional carbon nanotubes with a greater thermal conductivity (k), directly converting chemical energy into electricity.^{6–8} Once the exothermic chemical reaction was initiated, heat was transferred to the nanotubes and traveled along the nanotube length axis at a higher speed because of the greater value of k . Finally, the heat was fed back to the surrounding energetic material, resulting in a higher overall chemical reaction rate.^{6–8} However, the Seebeck coefficient (α) of carbon nanotubes is not high (~80 $\mu\text{V}/\text{K}$),^{6,9,10} limiting the generated electrical potential. Peak voltages have typically been about 30–50 mV, although a

maximum value as large as 210 mV was reported.^{6,10,11} Thermoelectric thin films with greater α values, such as n-type Bi₂Te₃, p-type Sb₂Te₃, and n-type ZnO films, were more recently investigated to increase the electrical potential.^{10–12} The thermoelectric thin films were placed on top of substrates with greater k values, such as alumina substrates, because the low k values of the thermoelectric thin films were unfavorable for maintaining thermopower waves.^{10–12} A maximum voltage output on the order of 500 mV was obtained with a ZnO thin film on an alumina substrate.¹²

We recently decoupled and enhanced both α and electrical conductivity (σ) by constructing a nanoscale Sb₂Te₃ film on monolayer graphene by a simple sputtering method.¹³ The Sb₂Te₃ crystal structure on graphene was aligned along the c axis, and the external graphene layer provided a highway for charge carriers due to the high mobility. The α and σ values of the heterostructure bilayer were enhanced by 38% (~324 $\mu\text{V}/\text{K}$),

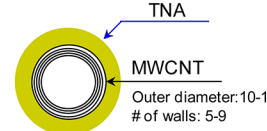
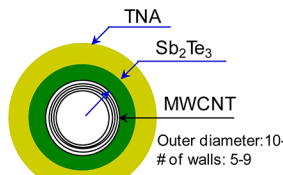
Received: November 28, 2012

Revised: December 16, 2012

Published: January 3, 2013



Table 1. Schematics and Notation of Synthesized Specimens

Sample configuration	Layer 1	Layer 2	Layer 3	Notation
 Outer diameter: 10-12 nm # of walls: 5-9	MWCNT	TNA	-	MWCNT/TNA
 Outer diameter: 10-12 nm # of walls: 5-9	MWCNT	Sb ₂ Te ₃	-	MWCNT/Sb ₂ Te ₃
	MWCNT	Sb ₂ Te ₃	TNA	MWCNT/Sb ₂ Te ₃ /TNA

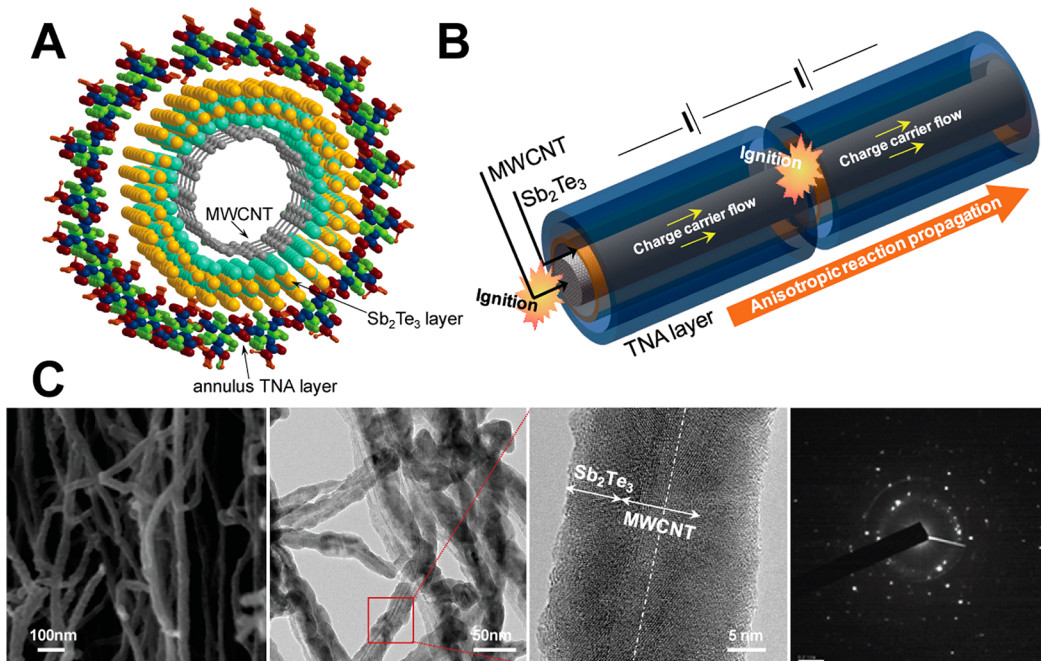


Figure 1. MWCNTs coated with Sb₂Te₃ and TNA: (a) Schematic of MWCNT/Sb₂Te₃/TNA. (b) Serial connection of two MWCNT/Sb₂Te₃/TNA units. (c) Scanning electron microscopy (SEM; JEOL, JSM7500F instrument), transmission electron microscopy (TEM; JEOL, JEM 2100F instrument), and selected-area electron diffraction (SAED) images of MWCNT/Sb₂Te₃.

K) and 87% (820 S/cm), respectively, compared with those of a pure Sb₂Te₃ film on a Si–SiO₂ substrate.¹³ Here, we report Sb₂Te₃-coated multiwalled carbon nanotube (MWCNT) arrays to enhance the α value of the thermoelectric compound. The suspended one-dimensional tube arrays eliminate thermal interference with substrates that could be operating for supported thermoelectric thin films. The electrical potential could be significantly enhanced when the multishell structure was coupled with the exothermal chemical reaction of cyclotrimethylene trinitramine (TNA).

EXPERIMENTAL SECTION

Synthesis of Sb₂Te₃-Coated MWCNT Arrays. Vertically aligned MWCNTs ($5 \times 5 \times 5$ mm³) were synthesized by chemical vapor deposition in a horizontal tube furnace with an inner diameter of 2.9 cm. Detailed synthesis conditions were published previously,^{14–16} and a brief description is provided

here. Layers of Fe (1 nm) and Al₂O₃ (20 nm) were deposited on a Si–SiO₂ substrate by an electron beam evaporation method. The reactor was heated to 750 °C in 15 min while being purged with Ar (180 ± 10 sccm). Catalyst particles were formed by injecting a mixture of Ar and H₂ (57 ± 5 sccm) for 10 min. In the next step, C₂H₄ (25 ± 3 sccm), Ar (180 ± 10 sccm), and H₂ (57 ± 5 sccm) were introduced into the tube furnace to grow nanotubes. Finally, the tube furnace was cooled to room temperature.

The MWCNT array was sliced into thin films with a thickness of ~200 μm, and Sb₂Te₃ was sputtered on the thin films by a magnetron sputtering method at an elevated substrate temperature of 473 K.^{13,17} The chamber pressure was 3×10^{-3} Torr, and an Sb₂Te₃ alloy target was sputtered at a radio-frequency power of 30 W.¹³

Wet Impregnation of TNA. TNA (C₃H₆N₆O₆) in acetonitrile (110 mM, 50 μL) was impregnated into the

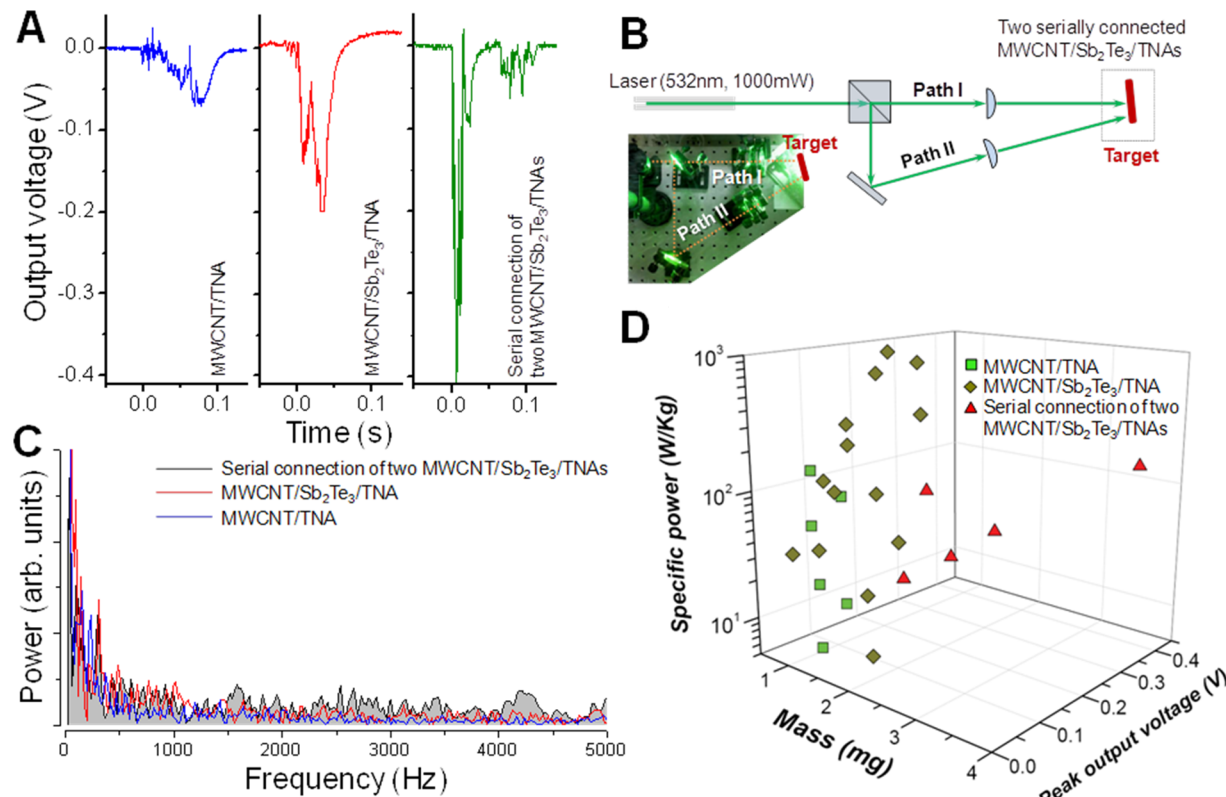


Figure 2. (a) Thermopower waves generated from MWCNT/TNA, MWCNT/Sb₂Te₃/TNA, and the serial connection of two MWCNT/Sb₂Te₃/TNA units. (b) Schematic of the laser beam steering optics for the simultaneous ignition of two serially connected MWCNT/Sb₂Te₃/TNA units. (c) FFT analysis. (d) Specific powers as a function of mass and peak voltage.

Sb₂Te₃-coated MWCNT array⁶ and dried for several hours under ambient conditions. A NaN₃ aqueous solution (3 mM, 10 μ L) was also added as a primary igniter because it has a lower activation energy.⁶ Finally, the thin films were cut into segments of aligned nanotubes with a length of 5 mm and varying widths of 1–2 mm. The notation for the synthesized specimens is summarized in Table 1.

Characterization of Thermopower Waves. The energetic compound (MWCNT/TNA or MWCNT/Sb₂Te₃/TNA) was connected to copper electrodes using silver paste and excited by laser irradiation (Shanghai Dream Laser Co., 532 nm, 1000 mW). The thermopower wave was monitored using an oscilloscope (Agilent, DSO5014A). The serial connection was also constructed by combining two segments of MWCNT/Sb₂Te₃/TNA units using silver paste. There was some variation in peak voltages and wave durations even for the same type of sample, probably because of the nonuniform nature of the sputter-deposited Sb₂Te₃ on the nanotubes, the TNA/NaN₃ coating obtained by the wet-impregnation method, the laser-irradiated spots, and the silver-pasted contacts.

RESULTS AND DISCUSSION

A schematic of the multishell structure is shown in Figure 1a. An MWCNT was first surrounded by a Sb₂Te₃ layer followed by a TNA layer. A p-type Sb₂Te₃ layer was selected, rather than n-type, because the majority carriers in MWCNTs are holes.⁹ A parallel mixture of p-type and n-type materials diminishes the Seebeck effect because the concomitant movement of both electrons and holes cancels out the induced electrical potential.¹³ Sb₂Te₃ typically demonstrates high values of α (200–300 μ V/K) and σ (50–500 S/cm), although the precise

values depend on crystal structure and synthesis method.^{10,13} The low k value [\sim 2.5 W/(m K)] of Sb₂Te₃ was considered to be unfavorable for guiding thermopower waves because fast reaction propagation relies on a high k for the waveguide.^{6,10} However, the interfacial thermal resistance of the thin intermediate layer between the exothermic chemical reactant (TNA) and the nanotubes in this annular multishell configuration, arising from phonon scattering at the heterointerface and the low k value of Sb₂Te₃, has little effect on the wave propagation. A previously published modified Fourier's equation revealed that the interfacial thermal conductance beyond a minimum threshold becomes insignificant, as the radial heat exchange between shells is not rate-limiting because of the rapid thermal equilibrium in the narrow reaction front.⁶ Therefore, both the high α value of Sb₂Te₃ and the high k value of MWCNTs can be utilized to generate self-sustained thermopower waves with high electrical potentials. A serial connection of two repeating units was also designed to increase the resulting electric potential from thermopower waves (see Figure 1b).

For experimental implementation, MWCNT arrays were synthesized by chemical vapor deposition [see Figure S1 (Supporting Information) and the Experimental Section for details].^{14–16} The average number of walls was five to nine, with average inner and outer diameters of 6–8 and 10–12 nm, respectively. The length of the array was \sim 5 mm. In the next step, the array was sliced with a thickness of \sim 0.2 mm and coated with Sb₂Te₃ by a magnetron sputtering method.^{13,17} Sputter conditions identical to those used previously for the deposition of a 10-nm-thick Sb₂Te₃ layer on graphene¹³ were applied in this study. A further increase in the thickness of the

Sb_2Te_3 layer would diminish the role of the nanotube thermal conduit.¹⁰ A thermally conductive core is required to enhance the reaction propagation velocity and maintain thermopower waves.⁶ Although a complete symmetrical coating could not be achieved by the sputtering process, the tubes were partly surrounded by Sb_2Te_3 because of the multiple collisions of depositing molecules,¹⁸ as shown in the scanning electron microscopy (SEM) and transmission electron microscopy (TEM) images in Figure 1c. Selected-area electron diffraction (SAED) analysis revealed the polycrystalline nature of the MWCNT/ Sb_2Te_3 material.¹⁹ The tubes at the surface were relatively uniformly coated, as shown by energy-dispersive X-ray elemental mapping (see Figure S2, Supporting Information). The atomic ratio between Sb and Te was 1:1.5, demonstrating the stoichiometric composition. It is possible that the outer tubes were damaged during the sputtering process because of the momentum of depositing molecules.¹³ However, the relatively intact inner tubes with high k values should contribute to the acceleration of the reaction and the generation of thermopower waves along the length axis. Finally, MWCNT/ Sb_2Te_3 was coated with TNA by the wet-impregnation method.⁶

Figure 2a shows thermopower waves generated from MWCNT/TNA, MWCNT/ Sb_2Te_3 /TNA, and the serial connection of two MWCNT/ Sb_2Te_3 /TNA units. The size of MWCNT/TNA and MWCNT/ Sb_2Te_3 /TNA was $\sim 5 \times 0.2 \times (1-2)$ mm³. The typical peak voltage of MWCNT/TNA was ~ 72 mV. Two regions in the thermopower voltage signals, namely, the initial reaction and the subsequent cool-down zones, can be more clearly observed in a magnified graph similar to data in other publications (see Figure S3a, Supporting Information).^{6,10-12} The incorporation of the Sb_2Te_3 layer between MWCNT and TNA increased the maximum peak voltage by 175% (~ 198 mV) probably due to the enhanced α of MWCNT/ Sb_2Te_3 /TNA. It is interesting to note that this peak potential is very close to the previously reported peak voltage (200 mV) of the thermopower waves from an Sb_2Te_3 thin film on an alumina substrate.¹¹ Highly oscillatory voltage signals could also be observed (see Figure S3b, Supporting Information).

An analytical model was employed to estimate the α value of MWCNT/ Sb_2Te_3 /TNA because it is difficult to measure α for a single nanotube coated by Sb_2Te_3 without probe perturbation. A parallel array of two thermoelectric materials was assumed, and the interfacial effect between the two layers was neglected (see the Supporting Information for details).²⁰ The Seebeck coefficient of MWCNT/ Sb_2Te_3 is described by the equation²⁰

$$\alpha = \frac{\alpha_{\text{MWCNT}} R_{\text{Sb}_2\text{Te}_3} + \alpha_{\text{Sb}_2\text{Te}_3} R_{\text{MWCNT}}}{R_{\text{MWCNT}} + R_{\text{Sb}_2\text{Te}_3}} \quad (1)$$

where R is the resistance. The subscript indicates the material of each component. The resistivity (ρ) was used to calculate R for the Sb_2Te_3 layer as $R = \rho L/A$, where A is the cross-sectional area and $L = 5$ mm is the length of the specimen. The following assumptions were used as an approximation: The outer diameter of the tube was 10 nm, and the thickness of the Sb_2Te_3 layer was uniform (10 nm). The α (234 $\mu\text{V/K}$) and ρ (22.7×10^{-6} $\Omega \text{ m}$) values of the 10-nm-thick Sb_2Te_3 film sputter-deposited on a silicon wafer were used for the calculation.¹³ The α (80 $\mu\text{V/K}$)^{6,9,10} and R (6 k Ω)²¹ values of an MWCNT were obtained from the literature. The

estimated α value of MWCNT/ Sb_2Te_3 (140 $\mu\text{V/K}$) increased by 75% compared with that of an MWCNT (80 $\mu\text{V/K}$). This increase is smaller than the observed enhancement in peak voltage ($\sim 175\%$). The difference could come from the nonuniform coating, interfacial effects, and different properties between the nanotubes in the literature^{6,9,10,21} and the CVD-grown tubes used in this study.

The serial connection of two MWCNT/ Sb_2Te_3 /TNA units was constructed using silver paste, and the two units were simultaneously excited by laser irradiation (Figure 2b). A laser source with a power of 1000 mW was divided into two beamlets using a beam splitter. Each beamlet was then focused on each end of the MWCNT/ Sb_2Te_3 /TNA using a plano-convex lens. The thermochemical reaction was almost instantly initiated upon irradiation of the laser because the ignition delay at a laser power of ~ 500 mW was very small. The thermopower waves were superimposed to increase the peak electrical potential to ~ 406 mV. Figure 2c shows the fast Fourier transform (FFT) analysis of the thermopower waves.⁷ The sampling frequency was 10000 Hz. The power generally increased when the Sb_2Te_3 layer was incorporated between the MWCNTs and the TNA because of the increased voltage oscillation. An increase in high-frequency power ($\gtrsim 1500$ Hz) was apparent for the serial connection, compared with that of MWCNT/ Sb_2Te_3 /TNA, because these irregularly oscillating waves could not be perfectly synchronized. The area under the spectrum of the two serially connected MWCNT/ Sb_2Te_3 /TNA units is shaded for comparison.

Figure 2d compares the peak specific power as a function of the peak voltage and mass of energetic compounds. The peak specific power increased with increasing peak voltage, and the maximum value for MWCNT/ Sb_2Te_3 /TNA was ~ 0.93 kW/kg. This value is slightly greater than the peak power (~ 0.6 kW/kg) of the thermopower waves from an Sb_2Te_3 film on an alumina substrate.¹¹ It is possible that the total resistance decreased as a result of the contribution of highly conductive MWCNTs because the thickness of the Sb_2Te_3 layer was only ~ 10 nm in this multishell structure. The total resistance increased for the serial connection because of the resistances from two units and the contact formed by silver paste. Consequently, the peak specific power of two serially connected MWCNT/ Sb_2Te_3 /TNA units was not greater than that of the single unit despite the enhanced electrical potential.

CONCLUSIONS

In summary, the incorporation of an Sb_2Te_3 layer between MWCNTs and TNA enhanced the maximum electrical potential by 175% (~ 198 mV) compared with that of MWCNT/TNA. An analytical model predicted an enhancement in α by $\sim 75\%$ compared with the value for a pure MWCNT. Both the high α value of Sb_2Te_3 and the high k value of the MWCNTs could be utilized in the multishell design to generate self-sustained thermopower waves with high electrical potentials. The peak potential increased to ~ 406 mV when two MWCNT/ Sb_2Te_3 /TNA units were joined together in series. However, there was no increase in specific power because of the resistance from two units and the contact interface.

ASSOCIATED CONTENT

S Supporting Information

Microscope images of vertically aligned MWCNTs, energy-dispersive X-ray elemental mapping of MWCNT/ Sb_2Te_3 , thermopower wave voltage profiles, and analytical model.

This material is available free of charge via the Internet at
<http://pubs.acs.org>.

■ AUTHOR INFORMATION

Corresponding Author

*E-mail: sbaik@me.skku.ac.kr. Tel.: +82-31-290-7677. Fax: +82-31-290-5889.

Notes

The authors declare no competing financial interest.

■ ACKNOWLEDGMENTS

This research was supported by the Basic Science Research Program (2011-0004463), the WCU (World Class University) program (R31-2008-000-10029-0) through the NRF of Korea funded by MEST, and the Human Resources Development program (No. 20124010203270) of the KETEP grant funded by the Korean government Ministry of Knowledge Economy.

■ REFERENCES

- (1) Choi, C. Q. *Sci. Am., Int. Ed.* **2006**, *294*, 72–79.
- (2) Loreto, M.; Francesc, M. *Proc. SPIE* **2005**, *5837*, 359–373.
- (3) Baxter, J.; Bian, Z.; Chen, G.; Danielson, D.; Dresselhaus, M. S.; Fedorov, A. G.; Fisher, T. S.; Jones, C. W.; Maginn, E.; Kortshagen, U.; Manthiram, A.; Nozik, A.; Rolison, D. R.; Sands, T.; Shi, L.; Sholl, D.; Wu, Y. *Energy Environ. Sci.* **2009**, *2*, 559–588.
- (4) Snyder, G. J.; Toberer, E. S. *Nat. Mater.* **2008**, *7*, 105–114.
- (5) Rowe, D. M. *Thermoelectrics Handbook: Macro to Nano*; CRC Press: Boca Raton, FL, 2006.
- (6) Choi, W.; Hong, S.; Abrahamson, J. T.; Han, J. H.; Song, C.; Nair, N.; Baik, S.; Strano, M. S. *Nat. Mater.* **2010**, *9*, 423–426.
- (7) Abrahamson, J. T.; Choi, W.; Schonenbach, N. S.; Park, J.; Han, J. H.; Walsh, M. P.; Kalantar-zadeh, K.; Strano, M. S. *ACS Nano* **2011**, *5*, 367–375.
- (8) Choi, W.; Abrahamson, J. T.; Strano, J. M.; Strano, M. S. *Mater. Today* **2010**, *13*, 22–33.
- (9) Kim, P.; Shi, L.; Majumdar, A.; McEuen, P. L. *Phys. Rev. Lett.* **2001**, *87*, 215502.
- (10) Walia, S.; Weber, R.; Latham, K.; Petersen, P.; Abrahamson, J. T.; Strano, M. S.; Kalantar-Zadeh, K. *Adv. Func. Mater.* **2011**, *21*, 2072–2079.
- (11) Walia, S.; Weber, R.; Sriram, S.; Bhaskaran, M.; Latham, K.; Zhuiykov, S.; Kalantar-Zadeh, K. *Energy Environ. Sci.* **2011**, *4*, 3558–3564.
- (12) Walia, S.; Weber, R.; Balendhran, S.; Yao, D.; Abrahamson, J. T.; Zhuiykov, S.; Bhaskaran, M.; Sriram, S.; Strano, M. S.; Kalantar-Zadeh, K. *Chem. Commun.* **2012**, *48*, 7462–7464.
- (13) Hong, S.; Kim, E. S.; Kim, W.; Jeon, S.-J.; Lim, S. C.; Kim, K. H.; Lee, H.-J.; Hyun, S.; Kim, D.; Choi, J.-Y.; Lee, Y. H.; Baik, S. *Phys. Chem. Chem. Phys.* **2012**, *14*, 13527–13531.
- (14) Kim, H.; Chun, K. Y.; Choi, J.; Kim, Y.; Baik, S. *J. Nanosci. Nanotechnol.* **2010**, *10*, 3362–3365.
- (15) Kim, H.; Lee, C.; Choi, J.; Chun, K. Y.; Kim, Y.; Baik, S. *J. Korean Phys. Soc.* **2009**, *54*, 1006–1010.
- (16) Yoon, D.; Lee, C.; Yun, J.; Cha, B. J.; Baik, S. *ACS Nano* **2012**, *6*, 5980–5987.
- (17) Jeon, S. J.; Oh, M.; Jeon, H.; Kang, S. D.; Lyeo, H. K.; Hyun, S.; Lee, H. J. *J. Electrochem. Soc.* **2011**, *158*, H808–813.
- (18) Madou, M. J. *Fundamentals of Microfabrication: The Science of Miniaturization*, 2nd ed.; CRC Press: Boca Raton, FL, 2002.
- (19) Andrews, K. W.; Dyson, D. J.; Keown, S. R. *Interpretation of Electron Diffraction Patterns*, 2nd ed.; Adam Hilger: London, 1971.
- (20) Lyeo, H.-K.; Khajetoorians, A. A.; Shi, L.; Pipe, K. P.; Ram, R. J.; Shakouri, A.; Shih, C. K. *Science* **2004**, *303*, 816–818.
- (21) Dresselhaus, M. S.; Dresselhaus, G.; Avouris, P. *Carbon Nanotubes: Synthesis, Structure, Properties and Applications*; Springer: New York, 2001.